Aggregation of Hydrophobically End-Capped Poly(ethylene oxide) in Aqueous Solutions. Fluorescence and Light-Scattering Studies

E. Alami, M. Almgren,* and W. Brown

Department of Physical Chemistry, University of Uppsala, Box 532, S-751 21 Uppsala, Sweden

J. François

Institut Charles Sadron CNRS-ULP, 6 Rue Boussingault, 67083 Strasbourg Cedex, France

Received August 11, 1995; Revised Manuscript Received December 11, 1995[⊗]

ABSTRACT: The association of a monodisperse model associative polymer, hydrophobically end-capped poly(ethylene oxide), denoted $C_{12}EO_{460}C_{12}$, in aqueous solution has been studied. The macroscopic properties have been investigated by rheological methods and correlated to properties on the microscopic level, as revealed from fluorescence and light scattering. The $C_{12}EO_{460}C_{12}$ polymer associates in water through its hydrophobic end groups and gives rise to a sharp increase in viscosity at about 2×10^{-2} g mL^{-1} due to formation of large aggregates or networks. The aggregation starts, however, at much lower concentrations. Already at 0.5×10^{-2} g mL^{-1} hydrophobic domains large enough to dissolve pyrene have formed. The aggregation process is very gradual without a distinct cmc. An estimate of the aggregation number of the hydrophobic domains obtained from fluorescence is about 15−30 end groups per micelle. The distribution of relaxation times from DLS shows three important diffusive modes in the concentration range 3×10^{-3} to 5×10^{-2} g mL^{-1}. A fast mode in the dilute region is attributed to unimers or small oligomeric aggregates of $C_{12}EO_{460}C_{12}$. At concentrations near the point where the viscosity rises an intermediate mode appears. This mode is considered to reflect the cooperative motions of the formed network. In the whole concentration range studied a slow mode is present. In the dilute region this mode dissappears completely upon addition of salt and is therefore attributed to the PEO interchain interaction. In the high-concentration region, however, this mode is probably also influenced by the aggregation of the hydrophobic ends of $C_{12}EO_{460}C_{12}$. The validity of these results is discussed and compared with a model considering the gain/loss of free energy upon formation of aggregates (loops, oligomeric aggregates, and micelles).

Introduction

The properties of aggregates formed by associating polymers in aqueous solution have attracted widespread interest in recent years. This group of polymers, which are used as rheology control agents in water-based surface coatings, include traditional thickeners such as polyacrylates and cellulose derivatives, but also ethylene oxide−urethane copolymers (HEUR), which are highly efficient[1−4] thickeners even at relatively low molecular weights. The high efficiency depends both on the polymer−polymer interactions due to the presence of the hydrocarbon tails and on the interactions with other components in the coating formulation such as latexes and surfactants.[4−7] Although the polymers have been extensively studied, there is still a dearth of information concerning the size, the shape, and the connectivity of the polymer aggregates and the micelle-like hydrophobic microdomains formed in the systems, functioning as dynamic cross-links of polymers associated into a network.

Most of the early studies of HEUR thickeners were concerned with rheological measurements mainly giving information about the macroscopic properties of the solutions.[1,5−6,8,9] Recently, numerous more fundamental studies have been carried out on both binary (polymer−water) and ternary (polymer−water−surfactant) systems, using techniques such as static and dynamic fluorescence,[10−15] light scattering,[16−18] surface tension,[16] and NMR self-diffusion.[18−20] However, most of these studies were made on HEUR samples prepared by polycondensation of poly(ethylene oxide) (PEO) of low molecular weight in the presence of a diisocyanate and a long alkyl chain mono-alcohol. Such a synthesis method leads to polydisperse compounds with a multimodal molecular weight distribution, as determined by size exclusion chromatography (SEC).[6,16] The associative behavior of such polymers, characterized by a wide variation of the hydrophobicity, is difficult to interpret. In particular, it appears[14−16] as if the concentration region where the formation of micelle-like microdomains takes place is much broader than for low diblock molecular weight surfactants.

From a fundamental point of view, it seems more interesting to study model polymers of low polydispersity index which can be prepared by a direct modification of the hydroxyl groups of PEO. Alami et al.[21] described the synthesis of such model compounds and carefully characterized them by NMR, UV spectroscopy, and SEC. A systematic study of the structure of the concentrated aqueous solutions (C_p > 2 wt % or more depending of the polymer) by small-angle X-ray scattering, SAXS,[22] and small-angle neutron scattering, SANS,[21] has been undertaken. It turns out that the paraffinic end groups are gathered into microdomains of spherical shape with a radius which appears to increase somewhat with increasing concentration. Moreover, the SAXS and SANS scattering intensity curves exhibit at least two peaks, indicating a local cubic or cubic order analogous to that described for solutions of diblock copolymers.[23] For lower molecular weights a

* To whom correspondence should be addressed.

[⊗] Abstract published in *Advance ACS Abstracts,* February 15, 1996.

0024-9297/96/2229-2229$12.00/0

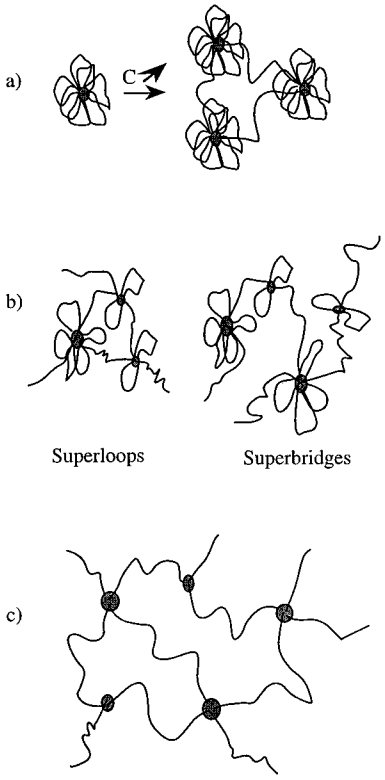

Figure 1. Schematic illustration of various possible states of chain association.

cubic mesomorphic phase is formed; up to five peaks are shown in the SAXS intensity curves, indicating a highly ordered structure.[22]

The same model samples have also been studied in the low-concentration range in order to investigate the onset of the association and to try to understand its mechanism. In particular, preliminary results[21] have shown that the micellization region is narrower than that observed with the polycondensed HEUR samples. The "critical micelle concentration" (cmc) has been studied as a function of molecular weight (M_w) and compared with the concentration at which the reduced viscosity abruptly diverges from that of the unmodified analogue. Such model polymers have also been synthetized by Abrahmsén-Alami et al. and studied by NMR relaxation,[24] self-diffusion,[24,25] and ESR[26] measurements.

At this stage of the investigations, a structural model of the aggregates able to give a good account of the whole sets of experimental observations is not quite clear. One can assume that at low concentrations the aggregates are of the "flower type", as schematized in Figure 1a, without connectivity between the hydrophobic microdomains. When the concentration exceeds the critical overlapping concentration of the "flowers", the connectivity through the PEO chains takes place progressively, explaining the abrupt rise of the viscosity. This picture is close to that recently presented by Semenov et al.[27] who predict a phase separation in the low concentration range between a dilute solution and a concentrated one which may be ordered. Their prediction is in qualitative agreement with the findings of Abrahmsén-Alami et al.[22] in the case of samples of $M_w = 2000$ and 4000 with two C_{12} end groups. Nevertheless, this is not the usual behavior of the so-called associative polymers which are generally soluble at low concentration. Annable et al.[28] have developed model taking into account the presence of micelles connected by "superbridges" or associated with "superloops" (Figure 1b) or "dangling ends". In both theories, the aggregation number (N_{agg}) of the micelles is assumed to be constant, in disagreement with SANS observations on model polymers which show that the size of the micelles increases upon increasing concentration,[29] but in agreement with results of Yekta et al.[14,15] indicating that N_{agg} does not depend on the concentration. One may remark that the model of Annable et al.[28] considers the presence of aggregates of low aggregation number (4) inside the superbridges and the superloops. This picture is then not too far from the simple approach of Maechling-Strasser et al.[17] who have explained the association by a simple model of open association governed by an association constant (Figure 1c). In this case, intermolecular association is favored over intramolecular (flowers).

This paper aims to clarify the first steps of the association for a model polymer of $M_W = 20\,000$ carrying two paraffinic end groups of 12 carbon atoms. Various techniques have been used: static fluorescence and dynamic fluorescence providing information on the presence and formation of hydrophobic microdomains. In favorable cases these methods allow the determination of the aggregation number N_{agg} of the micelle-like microdomains. Light-scattering techniques have also been used and provide information on the size, form, dynamics, and interactions of the aggregates. Viscosity measurements serve to relate macroscopic properties to the microscopic properties deduced from the other techniques.

The interactions with nonionic surfactants have also been studied and will be reported separately.[30]

Experimental Section

The model associative polymer (polyethylene didodecylether) has the following simple chemical structure: ■〰■ where 〰 is a poly(ethylene oxide) chain (PEO) with molecular weight of about 20 000 and ■ is a paraffinic chain with 12 carbon atoms. It is denoted $C_{12}EO_{460}C_{12}$. This sample was synthesized and purified according to the method described in a previous paper.[21] The molecular weight and the polydispersity index M_w/M_n of the associative polymer were determined by SEC in tetrahydrofuran. The molecular weight of the PEO precursor was $M_w = 20\,800$ with $M_w/M_n = 1.01$, and that of $C_{12}EO_{460}C_{12}$ was 20 300 with $M_w/M_n = 1.02$. The degree of substitution was found to be 95 ± 2% through ^{13}C NMR measurements.[21] Moreover the content of residual hydroxyl groups was determined by UV spectroscopy after substitution by naphthyl isocyanate (quantitative reaction). It was found to be 6 ± 1%, in agreement with NMR results.

Pyrene (Py), dodecylpyridinium chloride monohydrate (DPC), and dimethylbenzophenone (DMBP), used in the fluorescence studies were purchased from Aldrich.

Static Fluorescence. Fluorescence spectra were measured on a Hitachi F-4010 spectrofluorometer between 350 and 500 nm. Pyrene was used as a fluorescent probe at 5×10^{-7} M, usually with excitation wavelength at 335 nm.

The vibronic fluorescence spectrum of pyrene exhibits five peaks denoted I−V. It is well-known that the ratio I/III of the intensities of the first to the third peaks correlates with the polarity of the immediate environment of the pyrene molecules.[31,32] It is equal to 1.8−1.9 in water and reaches 0.9 in nonpolar solvents. In the first set of experiments, I/III was measured as a function of polymer concentration in order to follow the association process and to determine an order of magnitude of the cmc, by analogy with low molecular weight surfactants.

In the second set of measurements, the aggregation number of the hydrophobic microdomains was determined from the decrease of the probe fluorescence as a function of the concentration, [Q], of an added fluorescence quencher. The

fluorescence intensity I_Q in the presence of quencher is, under a number of requirements,[33,34] given by

$$I_Q = I_0 \exp\left(-\frac{[Q]}{[M]}\right) \quad (1)$$

where I_0 is the fluorescence intensity in the absence of quencher and [M] is the concentration of micelles. [M] is directly obtained from the slope of a $\ln(I_Q/I_0) = f([Q])$ plot. The aggregation number N_{agg} may be calculated from

$$N_{agg} = \frac{c - \text{cmc}}{[M]} \quad (2)$$

where c is the total molar polymer concentration and cmc is used to approximate the concentration of free polymer. This method can be applied only if the distribution of probe and quencher in the micelles satisfies the Poisson statistics and is frozen on the fluorescence time scale.

Dodecylpyridinium chloride (DPC) was used as a quencher in the static quenching experiments. One of the important requirements for the validity of eq 1 is that the rate of quenching in the micelles, expressed by the value of the first-order quenching rate constant, k_Q, is fast compared to the lifetime τ_0 of the unquenched probe. In separate time-resolved measurements, it was found that $k_Q\tau_0 \approx 7$, indicating[34] that the resulting aggregation numbers were slightly underestimated (ca. 10%).

Dynamic Fluorescence Measurements. In normal micellar solutions the micelle aggregation number, N_{agg}, can be obtained from an analysis of the fluorescence decay curves, determined using a single photon counting setup which has been described previously.[35] Pyrene and dimethylbenzophenone (DMBP) were used as the fluorescence probe P and quencher Q, respectively. Two measurements were performed on each polymer solution: one with only pyrene at a very low concentration, $[P] \approx 5 \times 10^{-7}$ M, which gave the undisturbed fluorescence lifetime τ_0 in the micellar environment, and the second at the same low [P] and a quencher concentration [Q] comparable to the micelle concentration [M]. The determination of N_{agg} from fluorescence quenching measurements is based on the Infelta−Tachiya equation for quenching in monodisperse micelles.[36,37] The fluorescence decay curves obey the equation

$$I(t) = I(0) \exp(-A_2 - A_3[1 - \exp(-A_4 t)]) \quad (3)$$

where $I(t)$ and $I(0)$ are the fluorescence intensities at time t and $t = 0$, respectively, following excitation. A_2, A_3, and A_4 are time-independent parameters that are estimated, together with $I(0)$, by fitting eq 3 to the experimental data.

In the case where the distributions of probe and quencher over the micelles are frozen on the fluorescence time scale, the expressions for A_2, A_3, and A_4 are[38,39]

$$A_2 = k_0; \qquad A_4 = k_Q \quad (4)$$

$$A_3 = \frac{[Q]_m}{[M]} \quad (5)$$

where $k_0 = 1/\tau_0$ is the fluorescence decay rate constant of the probe in the micelles without quencher and at low pyrene concentration (no excimer formation), $[Q]_m$ and [M] are the molar concentrations of quencher in micelles and of micelles, respectively, and k_Q is the pseudo-first-order rate constant for intramicellar quenching of the fluorescence of the probe. N_{agg} was calculated from eqs 2 and 5.

The preparation of the samples for fluorescence measurements has been described earlier.[13] To dissolve pyrene completely in the hydrophobic microdomains, the solutions were stirred at least overnight before measurement. The DMBP concentration was chosen to be less than one DMBP molecule per micelle. The measurements were made on aerated samples. The lifetime τ_0 thus determined was affected by oxygen quenching, but it was shown that the oxygen quenching had no effect on the determination of the aggregation number.

Dynamic Light-Scattering Measurements (DLS). The scattering cells (10-mL cylindrical ampules) were immersed in a large-diameter thermostated bath of index-matching liquid (transdecalin). The polarized (VV) DLS measurements in the self-beating (homodyne) mode were performed using a frequency-stabilized Coherent Innova Ar ion laser operating at 488 nm with adjustable output power. A typical laser power was 25 mW for the polarized data of the higher concentrations. The light was vertically polarized with a Glan-Thompson polarizer, with extinction better than 10^{-6}.

The detector optics employed a 4-μm-diameter monomodal fiber coupled to an ITT FW130 photomultiplier, the output of which was digitized by an ALV-PM-PD amplifier-discriminator. The signal analyzer was an ALV-5000 digital multiple-τ correlator (Langen GmbH) with 288 exponentially spaced channels. It has a minimum real time sampling time of 0.2 μs and a maximum of about 100 s. The intensity autocorrelation function, $g^{(2)}(t)$, was measured at different angles. In the present study the temperature was 25 °C where not otherwise indicated.

Data Analysis. The DLS data were analyzed by nonlinear regression procedures. The various models used in the fitting procedures are expressed with respect to $g^{(1)}(t)$, while the fitting was performed with respect to the measured $g^{(2)}(t)$, described as

$$g^{(2)}(t) - 1 = \beta\, g^{(1)}(t)^2 \quad (6)$$

where β is a nonideality factor which accounts for the deviation from ideal correlation. The autocorrelation function $g^{(1)}(t)$ can be written as the Laplace transform of the distribution of relaxation rate $G(\Gamma)$:

$$g^{(1)}(t) = \int_{-\infty}^{\infty} G(\Gamma) \exp(-\Gamma t)\, d\Gamma \quad (7)$$

where Γ is the relaxation rate and t is the lag time. For relaxation times, τ, eq 7 can be expressed as

$$g^{(1)}(t) = \int_0^{\infty} \tau A(\tau) \exp(-t/\tau)\, d \ln \tau \quad (8)$$

where $A(\tau) \equiv \Gamma G(\Gamma)$. $\tau A(\tau)$ was obtained by regularized inverse Laplace transformation (RILT) of the dynamic light scattering data using a constrained regularization calculation algorithm called REPES[40,41] as incorporated in the analysis package GENDIST. This algorithm directly minimizes the sum of the squared differences between experimental and calculated $g^{(2)}(t)$ functions. It allows the selection of a "smoothing parameter", *probability to reject*—the higher the *probability to reject*, the greater the smoothing. A value of 0.5 was chosen as standard in all analysis.

For light-scattering measurements, the solutions were mainly prepared in distilled water and sometimes in water + 0.25 wt % of sodium chloride and filtered using 0.45- or 0.20-μm Millipore filters.

Viscosimetry. Three viscosimeters were used according to the range of associative polymer concentration:

−for the low concentrations, $C_p < 10^{-2}$ g mL^{-1}, an automatic capillary viscosimeter of the Gramain−Libeyre type[42] (viscosimeter (Viscologic Sematech TI1) equipped with capillaries of 0.56- and 0.46-mm diameter).

−for concentrations between 5×10^{-3} and 5×10^{-2} g mL^{-1}, a low-shear Couette flow-type rheometer, Contraves LS30, working at shear rates from 0.017 to 128 s^{-1}.

−for concentrations higher than 2×10^{-2} g mL^{-1}, a Rheometer Rheostress RS100 from Haake which was used with different geometries: plane−plane 30 PP35, cone−plane C35/1 (30 mm, 1°), and a cylindrical cell double double gap of 55-mm diameter and 0.3- and 0.5-mm gap.

For the measurements of the viscosity in solutions of the unmodified PEO another capillary viscosimeter, a Ubbelohde, was used.

The apparatus was thermostated at 25 ± 0.05 °C.

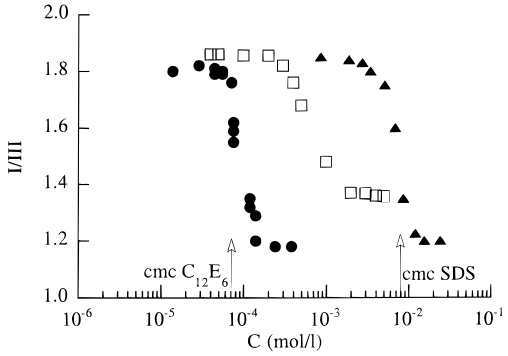

Figure 2. Variation of the intensity ratio I/III of the fluorescence pyrene spectrum in aqueous solutions of SDS (▲), $C_{12}E_6$ (●) and $C_{12}EO_{460}C_{12}$ (□) at 25 °C.

The reduced viscosity η_{red} of the polymer was calculated from the formula

$$\eta_{red} = \frac{\eta - \eta_0}{\eta_0 C_p} \tag{9}$$

where η and η_0 are the viscosities of the polymer solutions and the solvent, respectively, and C_p is the polymer concentration expressed in g mL^{-1}. The molar concentration will be denoted C.

Results

The associative polymer under study, $C_{12}EO_{460}C_{12}$, is soluble at room temperature and its lower critical solution temperature (LCST) in pure water is about 70 ± 2 °C.[21]

I. Fluorescence Measurements. Micellization Region (cmc). The I/III ratio of the intensities of the first and third vibronic peaks in the fluorescence spectrum of pyrene solubilized in $C_{12}EO_{460}C_{12}$ solutions was measured as a function of polymer concentration. In Figure 2, the results for this polymer are compared with those obtained for solutions of low molecular weight surfactants, ionic (SDS) and nonionic ($C_{12}E_6$).

The ratio I/III is an index of the polarity of the probe microenvironment. Since pyrene prefers the nonpolar regions very strongly—its water solubility is only about 5×10^{-7} M—the value of the ratio starts to decrease already at a very low volume fraction of the hydrophobic domains. Upon micellization, I/III generally decreases over a rather narrow concentration range, as exemplified for SDS and $C_{12}E_6$ in Figure 2. The change of the I/III ratio for the surfactants starts well before the cmc (as determined by other methods, *e.g.* surface tension), indicating that hydrophobic aggregates form at concentrations much lower than the cmc, at least in the presence of pyrene. The distribution of pyrene between water and micelles has been determined for some micellar systems.[43] For SDS the distribution constant was obtained as ca. 3×10^4 L/mol, implying that in 10^{-4} M surfactant in micellar form the transfer of pyrene to the micelles would be almost complete (75%). The results in Figure 2 for $C_{12}E_6$ suggest a distribution constant that is even larger, since already at a total surfactant concentration of 10^{-4} M the I/III value indicates a completely micellar microenvironment. The distribution is much less favorable for small aggregates, as expected for the polymers, and it is possible that a concentration of 0.5−1 mM of the polymer in the form of micellar aggregates is required before pyrene is mainly localized in them.

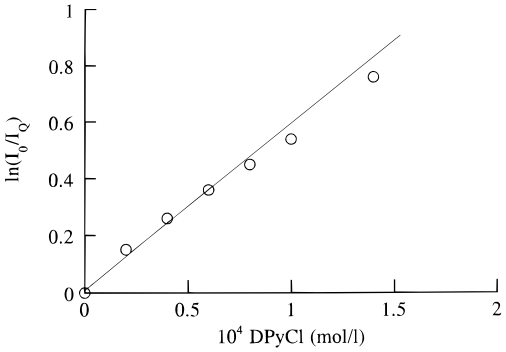

Figure 3. Plot of the fluorescence ratio I_0/I_Q for pyrene (6×10^{-7} M) quenched by dodecylpyridinium chloride (DPC) in an aqueous solution of $C_{12}EO_{460}C_{12}$ ($C_p = 5 \times 10^{-2}$ g/mL) at 25 °C.

For $C_{12}EO_{460}C_{12}$ the I/III transition occurs over a broad concentration range, from 2.5×10^{-4} M (5×10^{-3} g/mL) to 2×10^{-3} M (4×10^{-2} g mL^{-1}). It is not clear where the cmc—if there is one—is located. Comparison with I/III results for $C_{12}EO_{200}C_{12}$, for which a relatively well-defined cmc was obtained in calorimetric measurements,[25] suggests that the cmc should occur near 1.5×10^{-2} g mL^{-1}, or 0.75×10^{-3} M, *i.e.* close to the point of inflection of the I/III curve. Note that cmc = 8×10^{-3} M for SDS and cmc = 7×10^{-5} M for $C_{12}E_6$, also occur close to the inflection points (see Figure 2). The fact that the I/III value at concentrations above the cmc decreases only very slow toward 1.3, whereas normal surfactants give a I/III of 1.2 suggests that the hydrophobic domains are relatively small in the polymer solution. We shall return to the question of the significance of the I/III variation in the Discussion and for the moment use 0.75×10^{-3} M as the amount of polymer not involved in micelle-like aggregates at higher concentrations, a number needed to estimate the aggregation numbers from the fluorescence quenching results.

Aggregation Number. In normal surfactant solutions the aggregation number can be determined from static as well as dynamic fluorescence measurements. Figure 3 shows the results of static quenching experiments in a solution of the associative polymer ($C_p = 5 \times 10^{-2}$ g mL^{-1}). The pyrene concentration was sufficiently low that excimer formation could be neglected. The aggregation number obtained from the slope of the fit to the experimental data at low concentration, using 1.5×10^{-2} g mL^{-1} for the free polymer concentration (eqs 1 and 2) is $N_{agg} = 16$ chain ends ($C_{12}H_{25}$ groups) per micelle, assuming all quenchers (dodecylpyridinium chloride) to be associated with the micelles.

Parts a and b of Figure 4 show the fluorescence decay curves in aqueous solutions of the associative polymer in the absence and presence of quencher, respectively. For short times the decays were influenced by fluorescent impurities in the polymer preparation. The effects from this disturbance were minimized by increasing the pyrene concentration as much as possible without excimer formation. The remaining effect was corrected for using a procedure described in ref 35. The parameters used to calculate the aggregation number from eqs 4 and 5 were obtained by fitting eq 3 to the experimental data. The results are collected in Tables 1 and 2.

The static and time-resolved fluorescence quenching methods for the aggregation numbers primarily involve a determination of the fraction of excited pyrene in aggregates without quenchers. In the calculation of the aggregation numbers, it is assumed that both probes

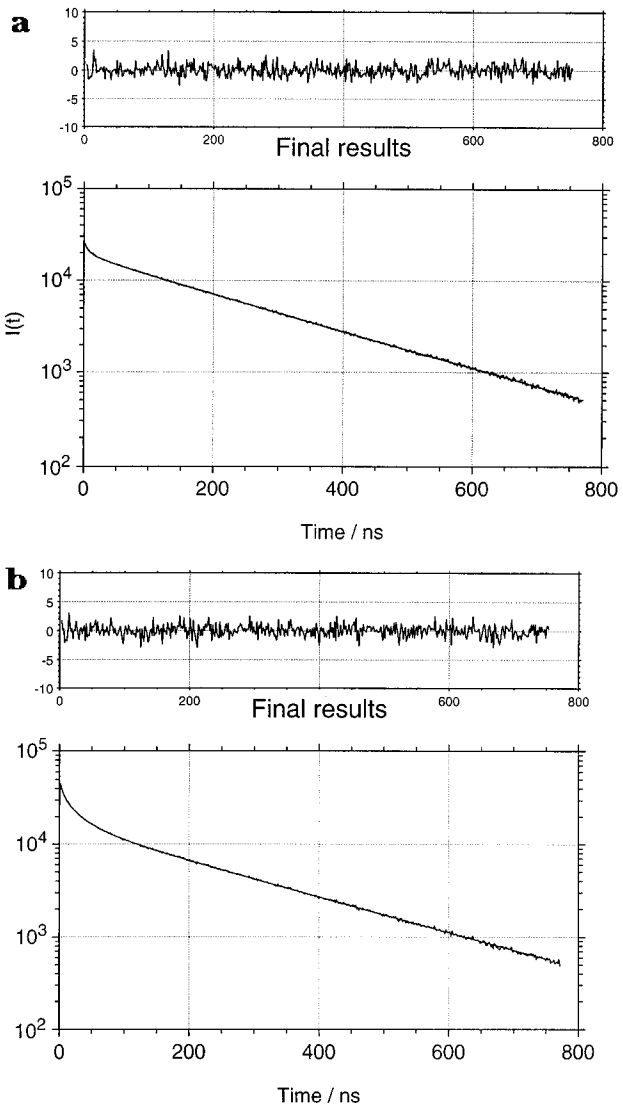

Figure 4. Fluorescence decay curves for pyrene in a solution of $C_{12}EO_{460}C_{12}$ (0.07 g/mL) in the absence (a) and the presence (b) of quencher (DMBP: 0.203 mM).

Table 1. Time-Independent Parameters As Obtained by Fitting Eq 3, Together with the Aggregation Number N_{agg} (of End Groups) As Determined Using the Experimental Data[a]

C_p (wt %)	τ_0 (ns)	A_3	$10^{-6}k_Q$ (s^{-1})	A_2^{-1} (ns)	N_{agg}	N^*_{agg}	[DMBP] (mM)
1.42	198.20	0.61	34.3	192.60		33	0.032
2.12	215.38	0.64	37.2	209.80	30	30	0.048
2.75	212.60	0.85	33.4	205.60	30	34	0.079
2.97	220.27	0.64	39.9	216.23	29	28	0.067
3.76	218.87	0.49	43.7	212.60	21	26	0.091
3.76	218.87	0.66	44.9	210.80	20	25	0.126
3.76	218.87	0.79	45.2	210.70	18	25	0.169
4.73	209.80	0.79	33.5	210.90	27	34	0.137
5.95	218.05	0.81	36.3	208.10	26	31	0.184
7.00	216.30	1.10	33.1	210.50	36	34	0.203

[a] N^*_{agg} is the aggregation number as evaluated from the aggregation number of $C_{12}E_8$ and the quenching rate constant.

and quenchers are randomly distributed over the aggregates (a Poisson distribution) so that the fraction of pyrene in micelles without quenchers is equal to $\exp(-n)$, where n is the average number of quenchers per micelle. The amounts of quencher, and surfactant or polymer, included in the micelles must be estimated. Usually, it is assumed that the concentration of free surfactant is equal to the cmc. As indicated above, we

Table 2. Time-Independent Parameters and the Aggregation Number of End Groups As Obtained by Fitting Eq 3 to the Experimental Data Using Pyrene Excimer Formation

C_p (wt %)	τ_0 (ns)	A_3	$10^{-6}k_Q$ (s^{-1})	A_2^{-1} (ns)	N_{agg}	[Py] (mM)
6.2	223.2	0.54	19.9	220.1	16	0.147
3.97	216.1	0.59	21.8	218.0	15	0.094

shall use $C_p = 1.5 \times 10^{-2}$ g mL^{-1}. To estimate the fraction of quencher in the micellar pseudophase, a value for the distribution constant, K_D, defined through

$$1.9K_D[P]_m = \frac{[Q]_m}{[Q]_{aq}} \qquad (10)$$

was taken from a determination of the distribution of the same quencher and the small micelles (about half the size of free micelles) formed by CTAC (cetyltrimethylammonium chloride) interacting with a polymer. This value, $K_D = 6 \times 10^2$ L/mol, is about 5 times smaller than the value obtained for free, normal size micelles of SDS and CTAB (cetyltrimethylammonium bromide).[44] The factor 1.9 in eq 10 is included to get the concentration of alkyl chain ends. This factor is also included in the aggregation numbers given in Table 1; it is the number of alkyl groups that are reported. Due to the uncertainty in the estimates of the concentrations of micelle-bound polymer and quencher, the aggregation numbers should be most reliable at high concentrations.

There are a number of points to be discussed concerning the results in Table 1. First of all, it is obvious that the aggregation does not suddenly start at a cmc; measurements from below the "cmc" give the same type of quenching, showing that hydrophobic domains are present; with the recipe used we cannot calculate an aggregation number for these. The aggregation numbers at higher concentrations vary without any trend. With the exceptions for an occasional low value of 21 and a high of 36, they are within 28 ± 3. The quenching constant varies around 3.6×10^7 s^{-1}, again without any trend. This pseudo-first-order quenching constant normally increases with the decreasing size of the micelle (for a discussion see ref 45)—some notable exceptions are micelles formed in interaction with polymers, and also aggregates formed in several HEUR thickeners, which seem to form very viscous cores.[13,14] Our model compounds seem to form normal cores, however, and if we assume that the product $k_Q N_{agg}$ is constant, the values determined for the quenching constant and aggregation number of $C_{12}E_8$ at 25 °C, $N_{agg} \approx 75$ and $k_Q \approx 1.5 \times 10^7$ s^{-1}, can be used for a calculation of aggregation numbers, N^*_{agg}, from the measured k_Q. The resulting values vary between 26 and 34 with a mean of 31, in good agreement with quenching aggregation numbers given in the table.

So far, the results show good consistency. The assumed distribution of the quencher between micelles and water implies, however, that the concentration of the quencher in the aqueous subphase is substantial and would lead to some quenching. A difference between the lifetime, τ_0, in the absence of quencher and the lifetime A_2^{-1} characteristic of the final exponential tail is also observed. The difference $A_2 - 1/\tau_0 = k_+[Q]_{aq}$, where the association rate constant for normal micelles is close to diffusion controlled, $k_+ \approx 5 \times 10^9$ L mol^{-1} s^{-1}.[43] The differences observed are in general smaller than what this relation would suggest, in particular at high polymer concentrations, suggesting that less of the

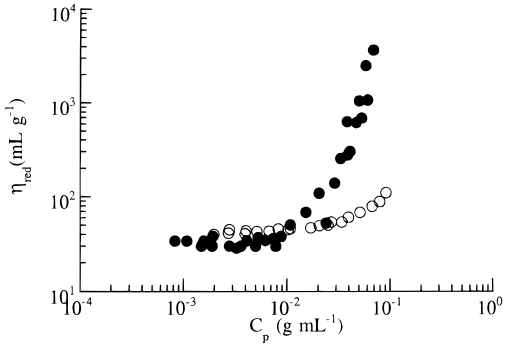

Figure 5. Variation of the reduced viscosity of $C_{12}EO_{460}C_{12}$ (●) and its unmodified homologue PEO (○) as a function of concentration in aqueous solutions at 25 °C.

quencher was free in the aqueous solution. Since this conclusion is based on differences that are not much larger than the errors in the lifetimes, it is not a strong indication that the quenchers are more strongly bound to the micelles (which would lead to smaller aggregation numbers). Finally, one solution ($C_p = 3.76 \times 10^{-2}$ g mL^{-1}) was measured at different quencher concentrations, which resulted in a slight decrease of the apparent aggregation number with increasing [Q] (Table 1), indicating that the conditions for a Poisson distribution of the quenchers over the micelles were not fully met. This could be due to polydispersity of the micelle size distribution,[45] but there could also be other reasons.[46]

To reduce the uncertainty due to the distribution of the quencher between the hydrophobic domains and water, a series of measurements was also performed using pyrene excimer formation to probe the fraction of pyrene present in micelles with only one pyrene molecule. In these experiments the pyrene concentration was high and the impurity emission negligible. The data were analyzed with eq 3, and the results are presented in Table 2. In this case A_2 is close to $1/\tau_0$; *i.e.* there is no significant migration and pyrene should be almost exclusively in the hydrophobic domains. The aggregation numbers are much smaller than obtained with DMBP, and in better accord with the result from the static quenching determination. It suggests either that DMBP is bound more strongly to the micelles than assumed or that the pyrene molecules avoid each other (which would give too small apparent aggregation numbers in Table 2), or that DMBP prefers micelles which already contain pyrene (too large apparent aggregation numbers in Table 1).

II. Viscosity. Figure 5 shows the variation of the reduced viscosity η_{red} of $C_{12}EO_{460}C_{12}$ and of its unmodified PEO analogue, in aqueous solutions. These results were obtained with the four different instruments as described in the Experimental Section. The two curves diverge at a polymer concentration of $(1-2) \times 10^{-2}$ g mL^{-1}—the scarce results in this region are too scattered to permit discrimination between a smooth change starting at 1×10^{-2} g/mL and a very sudden transition at around 2×10^{-2} g mL^{-1}—while a departure from the linear behavior for PEO is observed at $C_p = C_{p\eta_{PEO}} = 3 \times 10^{-2}$ g mL^{-1}. These values can be compared with the critical overlap concentration C^*_p of the unmodified PEO:

$$C^*_p = \frac{3M_w}{4\pi N R_g^3} \qquad (11)$$

where R_g is the radius of gyration. A value of (2.5−3) $\times 10^{-2}$ g mL^{-1} for C^*_p can be deduced from the empirical scaling laws describing the molecular weight dependence of Rg.[47,48] This value agrees with $C_{p\eta_{PEO}}$, but evidently the associative interactions of the modified chains start to affect the reduced viscosity prior to overlap of the unmodified chains. Either large, loose aggregates form, that give a big contribution to the intrinsic viscosity or, more likely, the viscosity increases due to bridging interactions between primary aggregates. Above a polymer concentration of $C_p \approx 2 \times 10^{-2}$ g mL^{-1}, the viscosity rises sharply, reminiscent of a percolative transition, which suggests that the transition point would be where an infinite network first forms. We shall return to a discussion of this view below.

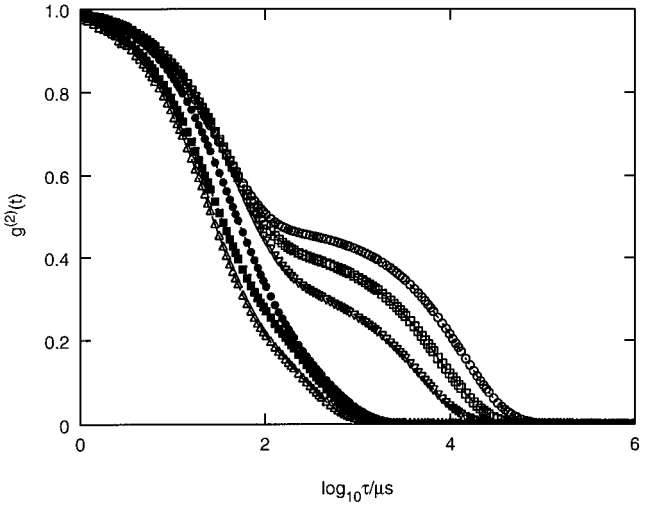

Figure 6. Time correlation functions $g^2(t)$ vs $\log(\tau)$ measured at $\theta = 90°$ for the aqueous solutions of $C_{12}EO_{460}C_{12}$: from the bottom to the top $C_p = 3.65 \times 10^{-3}$, 9.35×10^{-3}, 1.72×10^{-2}, 3.90×10^{-2}, 4.52×10^{-2}, and 5.16×10^{-2} g/mL.

At low concentrations the viscosity of the modified polymer falls below that of PEO. The intrinsic viscosity, obtained by extrapolating η_{red} to $C = 0$, has a slightly lower value (35 ± 2 mL g^{-1}) for the associative polymer than for PEO (41 ± 2 mL g^{-1}). It is well-known that a ring-shaped molecule has smaller dimension than the linear homologue. Casassa[49] has shown that the ratio of the intrinsic viscosities is 0.66, a result confirmed from measurements on model macrocyclic polystyrenes.[50] If the associative polymers were closed to loops, the intrinsic viscosity should be $41 \times 0.66 = 27$ mL g^{-1}. The experimental value 35 mL g^{-1} is intermediate between those of linear and cyclic chains, which could mean that there is an appreciative degree of looping, but compact aggregates would also give low intrinsic viscosity. Jenkins[6] found that the intrinsic viscosities of a series of HEUR polymers carrying chains of 16 and 12 carbon atoms were about the same as for the PEO analogue, but the generally studied polymers of higher molecular weight for which the looping probability is lower.

III. Dynamic Light Scattering. Dynamic light-scattering experiments were performed over a broad range of concentration, below and above the cmc region as determined from static fluorescence measurements, at 25 °C. Figure 6 shows polarized intensity−intensity correlation functions $g^2(t)$ for a scattering angle $\theta = 90°$ and for various concentrations of $C_{12}EO_{460}C_{12}$ (from 3.65×10^{-3} to 5.2×10^{-2} g mL^{-1}). The solutions were prepared in pure water and were passed through 0.45-μm filters. The functions are clearly far from single

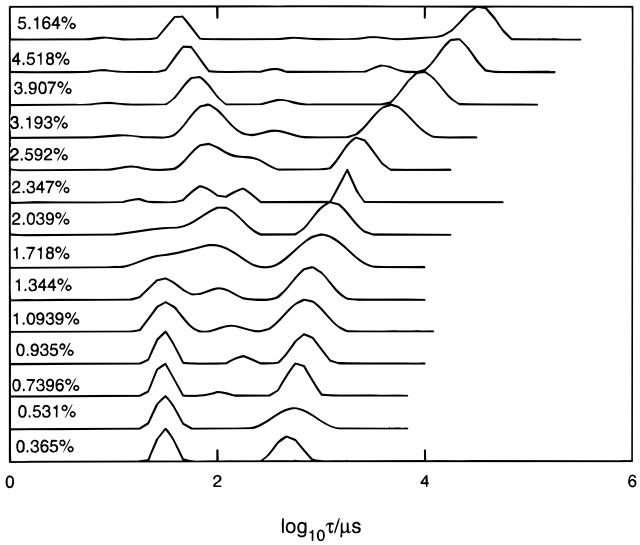

Figure 7. Decay time distributions corresponding to the data of Figure 6. The fast mode corresponds to the left peak and the slow mode to the right peak.

exponential. Distributions of relaxation times were obtained by analysis of the correlation functions by inverse Laplace transformation (ILT) using the algorithm REPES.[41] The evolution of these distributions with polymer concentration is shown in Figure 7. For concentrations lower than about $C_{pT_1} = 7 \times 10^{-3}$ g mL^{-1} (the first polymer transition T_1) they are bimodal, as is also the case for concentrations above about 1.3×10^{-2} g mL^{-1}. At intermediate concentrations, three modes are present. More precisely, for $C_{pT_1} < C_p < C_{pT_2} = 2 \times 10^{-2}$ g mL^{-1}, the fast and the slow modes are easily observable and the corresponding relaxation times vary weakly with concentration. The additional intermediate mode has an intensity which is an increasing function of concentration. For $C_p > C_{pT_2}$, the fast mode intensity decreases with increasing concentration. The relaxation time of the slow mode and its intensity increase with increasing concentration.

Figures 8 and 9 show that the relaxation rates of the fast Γ_f and the slow Γ_s modes are proportional to the square of the scattering vector ($q = 4\pi n_0 \sin(\theta/2)/\lambda_0$, where n_0 is the solvent refractive index, λ_0 is the wavelength, and θ is the scattering angle), demonstrating diffusive processes, according to

$$D = \frac{\Gamma}{q^2} \tag{12}$$

The corresponding plots for the middle mode are less convincing, but as shown in Figure 10 the value of the exponent, α, in the relation $\Gamma_m = q^\alpha$, is close to $\alpha \approx 2$ at all concentrations, indicating that this mode is also diffusive.

Low Concentrations, $C_p < C_{pT_1}$. Fast Mode. In the low-concentration range, the diffusion coefficient for the fast process, D_f, is almost constant; *i.e.* it is little affected by interparticle interactions. At infinite dilution, the hydrodynamic radius R_H is about 45 Å, according to

$$R_H = \frac{kT}{6\pi\eta D_0} \tag{13}$$

This value is close to that deduced from the empirical relationship of Devanand and Selser,[47] established for

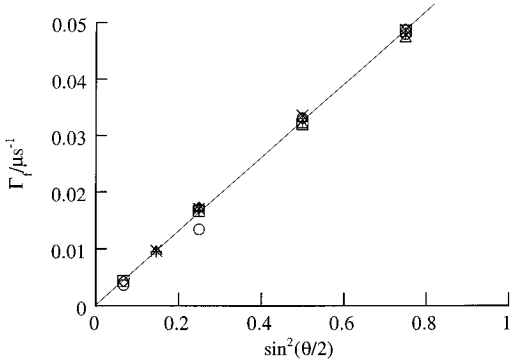

Figure 8. Plot of the relaxation rate of the fast mode, Γ_f, as a function of $\sin^2(\theta/2)$ at 25 °C for the aqueous solutions of $C_{12}EO_{460}C_{12}$ in the low concentration range: 3.65×10^{-3} (Δ), 5.31×10^{-3} (+), 7.40×10^{-3} (×), 9.35×10^{-3} (◇), 1.09×10^{-2} (□), 1.34×10^{-2} g/mL (ηop). The data are derived from the moments of the peaks corresponding to the maximum of the decay time distribution.

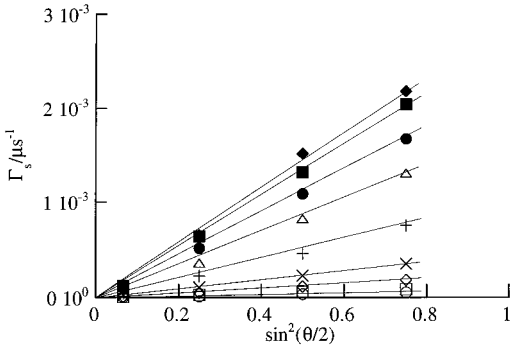

Figure 9. Plot of the relaxation rate of the slow mode, Γ_s, as a function $\sin^2(\theta/2)$ at 25 °C. For the aqueous solutions of $C_{12}EO_{460}C_{12}$ in the entire concentration range investigated: $C_p = 1.09 \times 10^{-2}$ (◆), 1.34×10^{-2} (■), 1.72×10^{-2} (●), 2.04×10^{-2} (Δ), 2.59×10^{-2} (+), 3.19×10^{-2} (×), 3.91×10^{-2} (◇), 4.52×10^{-2} (□), 5.16×10^{-2} g/mL (○). The data are derived from the moments of the peaks corresponding to the maximum of the decay time distribution.

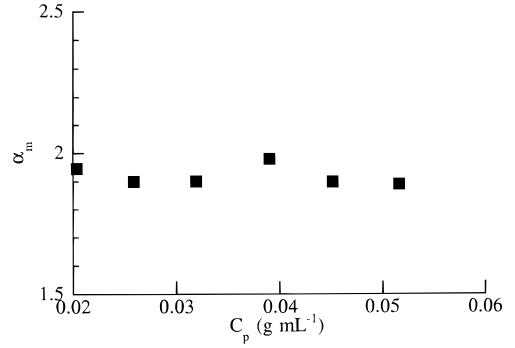

Figure 10. Power law exponent α_m, illustrating the q dependences of the intermediate mode.

unmodified PEO in water at 30 °C:

$$R_H = 0.145\, M_w^{0.571\pm0.009}\ (\text{Å}) \tag{14}$$

This relation gives $R_H = 42.4$ Å, for $M = 20\,000$; a similar value would be expected for the nonassociated modified polymer, if the effect of the end groups was negligible. Since D_f is independent of concentration, it seems to be little affected by interparticle interactions.

It is reasonable to conclude that in pure water, the fast mode at infinite dilution corresponds to unassociated molecules. The hydrodynamic radius of gyration of cyclic molecules would be $(0.66)^{1/3}$ of R_H for linear

molecules, and a value of 37 Å would be expected, which is lower than the experimental peak value (45 Å), but well within the experimental range. It is conceivable, therefore, that the solution contains some cyclic chains, in accord with the interpretation of the viscosity data. It cannot be excluded that the fast mode also contains very small clusters and/or oligomeric aggregates that cannot be distinguished from unimers.

Slow Mode. Extrapolation to zero concentration of the $D = f(c)$ curve for the slow mode gives $R_H \approx 490$ Å from eq 13, indicating that this mode may be attributed to polymer clusters. These measurements were made after filtration through a 0.45-μm filter. Another series of measurements was made with solutions filtered with a 0.20-μm filter and gave exactly the same value. Since the average size of the clusters is much smaller than the pore size of the filters used, this result is expected.

In the concentration range up to 2.5×10^{-2} g mL, both the fast and slow modes increase in intensity with increasing concentration (see Figure 13). It should be emphasized here that, although the slow and fast peaks have comparable amplitudes (Figure 11A, curve a in pure water), the weight concentration of the structures responsible for the slow mode will be small. At C_{pT_1}, the ratio of the diffusion coefficients D_f/D_s is approximately 10. The ratio of the weight concentrations is given by the relative amplitudes (here about 0.5) divided by the relative molar masses M_s/M_f. M_f/M_s is close to 1/55 using $D_f \propto M^{-0.57}$, and the relative weight concentrations C_s/C_f will thus be about 0.9×10^{-2}; the slow mode will thus be of marginal interest. It is obvious that the ratio $D_f/D_s = 10$ cannot be attributed to the formation of aggregates of the flower type: indeed, for a flower with $p = 70/2$ chains (70 being a typical aggregation number of surfactants with aliphatic tails of 12 carbons) the ratio D_f/D_s cannot exceed 3. This conclusion is based on the relation of Stockmayer and Fixmann[51] for starlike polymers of $n = N_{agg}$ branches:

$$g = \frac{3n - 2}{n^2} = \frac{R_{gb}^2}{R_{gl}^2} \tag{15}$$

where R_{gb} and R_{gl} are the radii of gyration of star and linear chains having the same molecular weight. For flowers of $p = n/2$ chains, the radii of gyration for the flower micelle and the unimer are related by

$$\frac{R_{gb}}{R_g} = \left(\frac{3n - 2}{n^2}\right)^{0.5}\left(\frac{n}{2}\right)^{0.571} \tag{16}$$

The hydrodynamic radius of the unimer should be close to that for a free coil, *i.e.* $R_H/R_g = 0.665$ according to Kirkwood et al.,[52] whereas the flower micelle is much more compact with the corresponding ratio approaching the limiting value of a hard sphere: $R_H/R_g = 1.29$. It follows

$$\frac{D_f}{D_b} < \frac{R_{gb}}{R_g}\frac{1.29}{0.665} \approx 3.06 \tag{17}$$

Finally, even if it is difficult to exactly determine the aggregation number and the shape of such aggregates, the combined results from fluorescence and light scattering are consistent with a small amount of large aggregates which do not contain large hydrophobic microdomains. Thus, this conclusion is in agreement with the appearance of such aggregates in a concentration range where the ratio I/III of the fluorescence spectrum of the pyrene remains close to that measured in water. The presence of a low concentration of clusters in the solution will not significantly affect the viscosity.

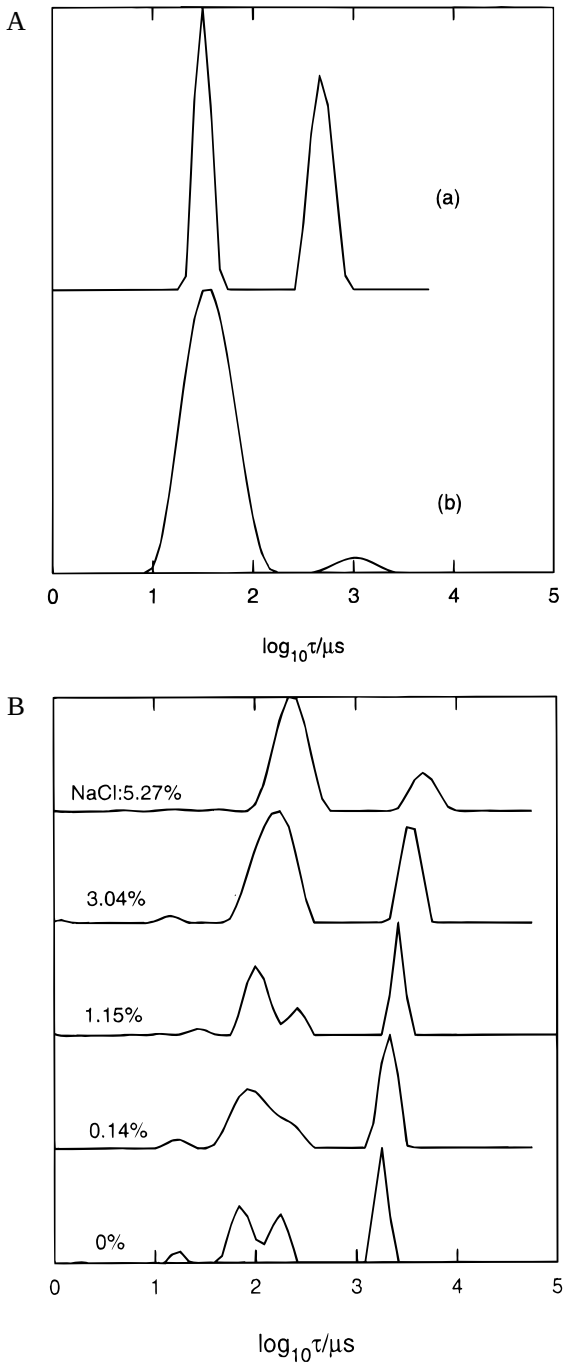

Figure 11. (A) Decay time distributions for $C_{12}EO_{460}C_{12}$ solutions ($C_p = 3.65 \times 10^{-3}$ g/mL) at scattering angle $\theta = 90°$ in pure water (a) and in the presence of 0.25 wt % of NaCl (b). (B) Effect of salt on the decay time distributions for $C_{12}EO_{460}C_{12}$ solutions ($C_p = 2.35 \times 10^{-2}$ g/mL) at scattering angle $\theta = 90°$.

The question arises whether the aggregates derive from simple experimental artifacts or whether they reflect the onset of the aggregation process. If the second hypothesis is correct, what are the respective roles played by the PEO chains and by their hydrophobic moieties in this process?

The presence of clusters in aqueous solutions of water-soluble macromolecules is not restricted to the associative polymers but has been the object of numerous investigations and controversial interpretations in the

cases of PEO, poly(1,3-dioxolane), and poly(vinyl alcohol), for example.[48,53−57] It is interesting to recapitulate some results obtained in static or dynamic light-scattering investigations performed on a PEO sample of the same molecular weight as the associative polymer under study (M = 20 000). While Strazielle[53] claimed that centrifugation can eliminate the aggregates from aqueous solutions if they are heated above the melting temperature of PEO, Polik and Burchard[54] have observed the presence of clusters even in centrifuged solutions. The latter authors showed enhancement of this phenomenon upon heating to 60 °C and a decrease of the apparent molecular weight above this temperature up to the phase separation. Recently, Devanand and Selser[55] have demonstrated the effectiveness of small pore size filters in eliminating aggregates, even in high molecular weight samples. More recently, Porsch et al.[55] came to a similar conclusion; they showed that the slow mode behavior is a result of the presence of an impurity, which can be removed by a solid phase extraction mechanism using hydrophobic filters. De Gennes[58] suggested that the association behavior described by Polik and Burchard has real physical significance and may correspond to phase separation between rich and poor polymer phases, in which the polymer chains remain expanded (Flory interaction parameter $\chi < 0.5$). Such a suggestion could reconcile the various experimental observations: filtration separates phases in thermodynamic equilibrium, and this separation cannot be obtained by simple centrifugation since the aggregates consisting of swollen chains are not sufficiently dense. A similar problem, but even more pronounced, exists with aqueous solutions of poly(1,3-dioxolane) (PDXL) where it has been shown that the anomalous excess scattered intensity disappears on addition of salt (0.01 N NaCl[48]). Although the explanation of this effect is not clear, it suggests that the presence of the clusters has physical significance. It was proposed that the sodium ions selectively occupy the binding sites, causing polymer aggregation, leading to the disentanglement of the chains which behave as repulsive polyions. This hypothesis is supported by several works which claim the formation of a "pseudo-polyelectrolyte" in the case of PEO through the interaction of the oxide group with various hydrated cations.[59] The binding constants of various cations with PEO have been obtained by Sartori et al.[60]

Recent papers of Nyström et al.[18] and Mortensen et al.[61] have discussed similar clustering phenomena at low concentrations in hydrophobically end-modified polymers, as reflected in dynamic light-scattering measurements. The tendency to form clusters would be greatly enhanced by the attractive interactions in hydrophobically-modified PEO, and we cannot exclude that the large aggregates at low concentrations are due to the same phenomenon as observed with unmodified PEO and not primarily to coupling between the hydrophobic end groups. For this reason, we have checked the influence of salt on the aggregation process in aqueous solutions of $C_{12}EO_{460}C_{12}$.

Figure 11A (trace b) illustrates the influence of 0.25 wt % of NaCl (4.3×10^{-2} M) on the distribution of the relaxation times for $C_p = 3.65 \times 10^{-3}$ g mL^{-1}. The slow mode almost disappears, and the fast mode is centered at the same value as in the distribution in pure water. If only hydrophobic interactions were responsible for the cluster formation in the very dilute regime, one would expect enhancement of this association on adding salt,

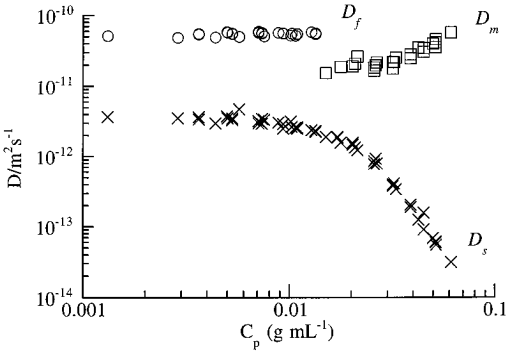

Figure 12. Concentration dependence of the diffusion coefficient of the fast mode (○), intermediate mode (□), and slow mode (×) at scattering angle $\theta = 90°$.

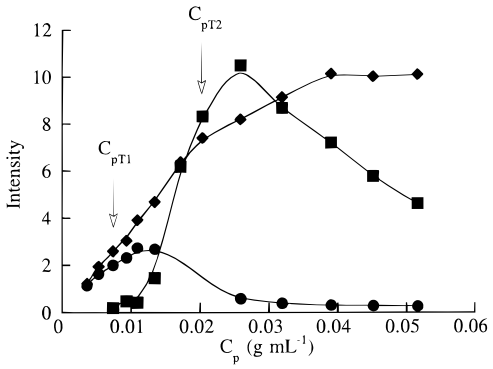

Figure 13. Concentration dependence of the fast (●), intermediate (■), and slow (◆) mode intensity for aqueous solutions of $C_{12}EO_{460}C_{12}$ at scattering angle $\theta = 90°$.

as recently shown by several authors[62,63] for nonionic associative polymers based on polyacrylamide. On the contrary, association due to the interchain PEO interaction disappears.

The effect of salt at high polymer concentrations (C_p = 2.35×10^{-2} g mL^{-1}) is shown in Figure 11B; in this case, the slow relaxation time distribution is less affected, showing that hydrophobic end-group interactions dominate the relaxation behavior in this concentration regime.

A systematic study of the behavior of these polymers in the presence of salt is beyond the scope of the present paper, but this preliminary result demonstrates its relevance. The broadening of the fast mode at low concentrations may arise because salt has two effects: the first leading to the breakdown of the PEO−PEO bonds responsible for the formation of large aggregates and the second enhancement of the hydrophobic interactions with formation of loops of smaller size or of flowers of larger size.

Intermediate and High Concentrations, $C_p > C_{pT_1}$. Figures 12 and 13, respectively, show the concentration dependences of the diffusion coefficients and of the intensities associated with the various modes over the range of concentrations investigated (note that Figure 12 contains data from several measurements using two different lasers). Above C_{pT_1}, the diffusion coefficient of the fast mode is approximately constant but its intensity decreases as C_p increases. One concludes that the number fraction of free polymer molecules (of the same size as exist in the very dilute regime) decreases progressively.

In the intermediate concentration range between about 1×10^{-2} and 2×10^{-2} g mL^{-1}, just before the

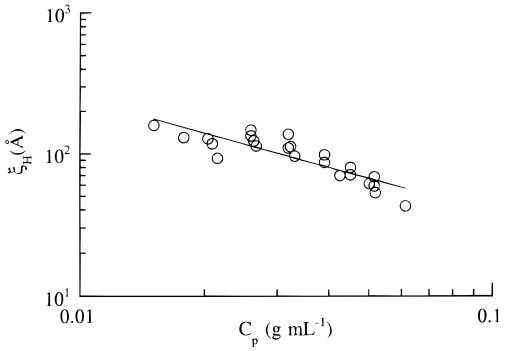

Figure 14. Concentration dependence of the correlation length ξ_H as obtained from the intermediate mode.

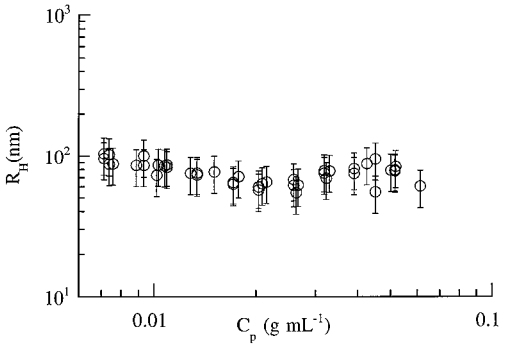

Figure 15. Concentration dependence of the hydrodynamic radius of the slow mode calculated from macroscopic viscosity measurements (error bars: 3 nm).

strong rise in the viscosity, DLS signals the emergence of an extensive network. The three modes are all clearly visible in Figure 7. It is of some interest to consider the size of aggregates that could give rise to such diffusive modes. We have already remarked that the ratio of $D_f/D_s = 10$ is too large to be consistent with flower-like micelles being responsible for the slow mode; the intermediate mode, however, gives a ratio $D_f/D_m \approx 2.5$, which is of the order of magnitude expected for flower micelles of relatively large aggregation number.

At higher concentrations the intermediate mode is considered to reflect the cooperative motions of the hydrophobic nodes which are interconnected by bridging polymer chains into a network. The screening of the hydrodynamic interactions is described by the hydrodynamic correlation length, $\xi = kT/6\pi\eta D_s$, which is shown as a function of concentration in Figure 14. ξ_H decreases smoothly with increasing concentration (a very approximate power law exponent is -0.8), indicating increased screening as the density of nodes increases. The intensity trace in Figure 13 reflects this change. With increasing concentration the number of hydrophobic microdomains increases, but eventually, as the network becomes more dense, the total scattered intensity decreases after passing through a maximum at about 2.5×10^{-2} g mL^{-1}.

In the high-concentration range, the slow mode is progressively slowed down, but if the macroscopic solution viscosity is used to estimate the hydrodynamic radius, the value remains constant, Figure 15. It is hard to imagine, however, that the loose aggregates that were argued above to be formed at low concentrations, primarily by nonhydrophobic interactions between the PEO chains, could remain at high concentrations when the network is well developed, and furthermore, the slow mode at high concentrations was unaffected by salt. It seems, therefore, as if the slow mode has a different origin at high concentrations and is a reflection of larger scale inhomogeneity in the network.

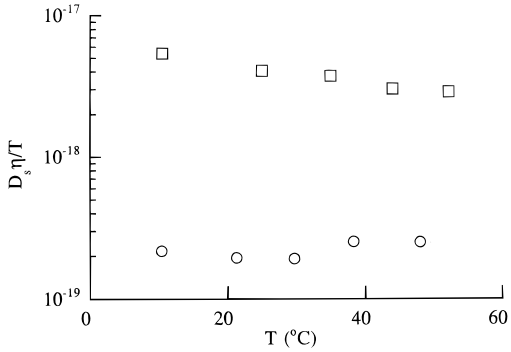

Figure 16. Temperature dependence of the slow diffusion coefficient at 5.02×10^{-2} (○) and 2.09×10^{-2} (□) g/mL polymer solution.

Temperature Dependence of the Diffusion. The temperature dependence of the slow mode was examined. The results for D_s at two polymer concentrations, $C_p = 5.02 \times 10^{-2}$ and 2.09×10^{-2} g mL^{-1}, are presented in Figure 16 as plots of the reduced diffusion coefficient: $D_s\eta/T$ vs T. This quantity is almost constant at high concentration but decreases slightly with increasing temperature at the lower concentration. This result is consistent with the formation of aggregates due to interactions between the PEO chains which become more attractive upon heating near the cloud-point temperature, as illustrated by the phase separation above 75 °C.

Discussion

Loops, Oligomeric Aggregates, and Micelles. The free-energy changes connected with the formation of a loop of an end-modified polymer have been discussed recently by several authors, using models developed for block copolymers.[64,65] There are two essential contributions for the isolated unimer: the loss of entropy when the polymer chain is back-folded and the gain in hydrophobic free energy when the two tails associate. The back-folding penalty was obtained from the probability that the two ends are close together: from general scaling arguments it was concluded that this probability should be proportional to $N^{-3/2}$ for a coil with N monomers following Gaussian statistics; we shall retain this form but also estimate the proportionality constant. The free energy of dimerization was estimated in the previous studies from the reduction of the interfacial free energy between the insoluble block and the solvent, assuming that already isolated blocks form spheres and fuse into one larger sphere. Such a treatment predicts a free energy of transfer to water which scales as $n_c^{2/3}$, where n_c is the number of carbons in the alkyl tail in our case. Since it is well-known that the free energy of transfer of alkyl groups to water, *e.g.* in processes such as micelle formation, depends linearly on n_c, implying that a single tail does not curl into a sphere, we prefer a different approach.

The back-bending probability can be estimated as the probability that the second end is within a distance a from the first one. The end distribution probability $p(r)$ is well-known for Gaussian chains, and we obtain

$$P(r<a) = \int_0^a 4\pi r^2 \left(\frac{3}{2\pi r_0^2}\right)^{3/2} \exp\left(-\frac{3r^2}{2r_0^2}\right) dr = \left(\frac{6}{\pi}\right)^{1/2}\left(\frac{a}{r_0}\right)^3 \quad (18)$$

If we put $r_0 = l_0 N^{1/2}$, and for simplicity choose $a = 2l_0$, we get

$$\Delta G_b^0 = -RT \ln P(r<2l_0) \approx -RT \ln\left(8\left(\frac{6}{\pi}\right)^{1/2}\right) + \frac{3}{2}RT \ln N = -2.6RT + 1.5RT \ln N \quad (19)$$

Apart from the constant term, this is the expression used earlier. An estimate of the hydrophobic effect on dimerization of the tails can be obtained from a comparison of the cmc values of single-tail and double-tail surfactants, or the differential free energy per CH_2 group from the change of the cmc on the addition of a CH_2 to the short tail of a double-tail surfactant, to the corresponding change for a single-tail surfactant. Some results of this type are available[66] and have been discussed by Tanford.[67] Other useful data, in particular for single-tail and double-tail zwitterionic compounds, are found in ref 68. The data suggest that the gain of free energy on association of the tails is between $0.3RT$ and $0.5RT$ per CH_2 group.

For our di-C_{12} PEO, the combined free energy of loop formation would amount to

$$\Delta G_l^0 \approx -(6.2 \text{ to } 8.6)RT + 1.5RT \ln 460 = (3.0 \text{ to } 0.6)RT \quad (20)$$

which means that the probability of loop formation would be about 0.05−0.035. In a good solvent for the middle block the looping tendency would be smaller and the polymer conformation more extended. We could expect, therefore, that the unimers form loops to some extent, in agreement with the results from the viscosity and DLS: with decreased length of the PEO chain or larger alkyl groups, loop formation would rapidly become more favorable.

In oligomeric aggregates of a few polymers, the back-bending penalty per chain would be about the same as for the unimers, but the hydrophobic effect would be much larger, so that dimers and trimers would be of the flower type almost exclusively.

For larger aggregates the stability of flower micelles versus micelles with dangling ends is a more complex question, since the repulsions of the soluble chains in the corona must be taken into account.[65] A simple way to estimate the probability of having dangling tails comes from a consideration of a process in which one tail is freed from the core of a flower micelle and replaced by a tail from a free unimer. In this process a micelle with two dangling ends is formed. The hydrophobic free energy is not affected, nor is the repulsive free energy in the corona, since the same number of half-polymers are associated. The main free-energy change comes from the release of the back-bending penalty and the confinement of the free monomer in the micelle. The equilibrium density, n, of unimers is then approximately given by

$$\frac{4\pi}{3}(a^3 n) = \left(\frac{6}{\pi}\right)^{1/2}\left(\frac{a}{r_0}\right)^3 \quad (21)$$

Insertion of $r_0 = 150$ Å (end-to-end distance) gives a unimer concentration of 1.6×10^{-4} M, which is in the range of the measured cmc values. As will be discussed below, however, the concentration of free unlooped unimers cannot reasonably be that high. One would expect, therefore, that the micelles have few dangling ends. It would not help for dangling ends to associate into pairs; the smaller loop formed by the free unimer would be preferred over that process. A larger hydrophobic effect, such as from a micellar core, is required to overcome the confinement free energy cost, so that bridging and the formation of multicentered networks, probably multiply connected, would be the next step in the aggregation process.

Let us now turn to the micelles and to a discussion of the effect of the long PEO chains on the cmc and the aggregation number. Let us first note that the free-energy gain when a tail is transferred from water to the micellar core is much larger than on dimerization; this is the very reason for the cooperativity in micelle formation. When many tails are in the core, it can be assumed spherical (but the number of tails must not be too large; more than about 60 C_{12} tails would lead to nonspherical shapes). For spherical micelles, the exposed surface area is proportional to $p^{2/3}$, where p is the aggregation number. The hydrophobic free energy of transfer per monomer, which drives the aggregation, would therefore vary as

$$\frac{\Delta G_{\text{hf}}^0}{RT} = -B_0 + B_1 p^{-1/3} \quad (22)$$

and would be the same, at a given p, for all monomers with the same tail length. B_0 and B_1, as well as B_2 introduced below, are positive constants. The repulsion between the head groups, or the free energy of the corona, limits the growth of the micelle and is responsible for the change of the cmc with the length of the hydrophilic EO_y part. In order to illustrate the effects of increasing the size of the EO block, we use an expression for the free energy of the corona given by Semenov et al.,[27] leading to the following expression for the free energy per unimer for micelle formation:

$$\frac{\Delta G^0}{RT} = -B_0 + B_1 p^{-1/3} + B_2 \ln y p^{1/2} \quad (23)$$

where y is the number of EO groups in the PEO part. We have used this free energy function to illustrate the change of the behavior from that of a normal nonionic surfactant, with $y = 8$, to a polymer with $y = 230$. The values of the B parameters were selected to give reasonable values of the aggregation number and the cmc for $C_{12}E_8$. B_1 is related to a surface free energy (the value chosen in the model calculations corresponds to 0.032 J m^{-2}) but is not the surface tension, since it contains also other effects that vary with the micelle size. In the calculations, values for the mole fraction, x_1, of free unimers were chosen, and the mole fraction of aggregates of p unimers was calculated from

$$x_p = x_1^p \exp\left(-\frac{p\Delta G^0}{RT}\right) \quad (24)$$

Figure 17 shows how the aggregation number and the concentrations of free monomer and monomer in micellar form change with the total concentration, using values of the parameters as stated in the legend. Note, that this simple model is not intended to be realistic; we only want to demonstrate how a large change of the repulsive interaction affects the aggregation number and onset of aggregation (an obvious defect of the model is the function chosen for the corona free energy, which is not valid for short chains and small aggregation numbers).

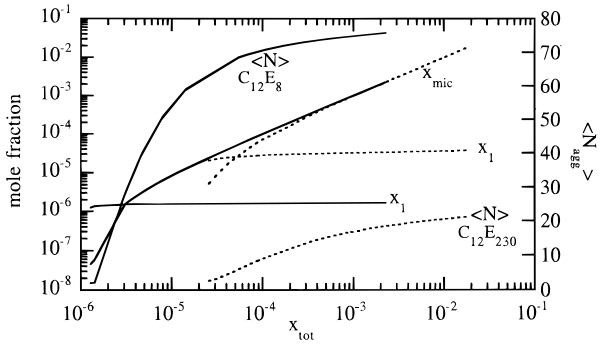

Figure 17. Average aggregation number $\langle N \rangle$, mole fraction of free unimers x_1, and mole fraction in aggregates x_{mic}, versus total mole fraction of $C_{12}E_8$ (solid lines) and $C_{12}E_{230}$ (dotted lines) according to the model of eqs 23 and 24. The parameter values are $B_0 = 20.3$, $B_1 = 18.9$, and $B_2 = 0.144$ in both cases.

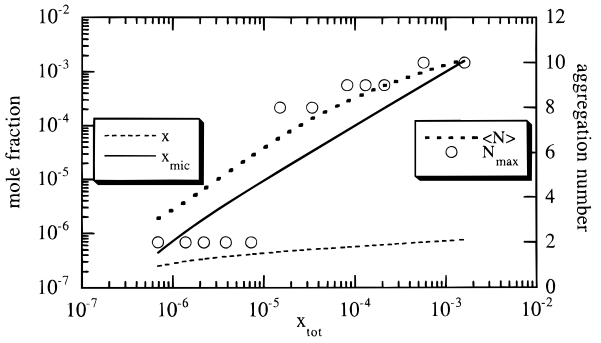

Figure 18. Average aggregation number, $\langle N \rangle$, the aggregation number of the most abundant species, N_{max}, and the mole fractions of free unimer, x_1, and of polymer in aggregates, x_{mic}, for $C_{12}EO_{460}C_{12}$, according to a model based on eqs 23 and 24. Parameter values: $B_0 = 34$, $B_1 = 30$, and $B_2 \ln y = 2.22$. These parameter values are compatible with the values used in Figure 17.

The model for $C_{12}E_8$ displays a behavior which is about as expected for micellization. The concentration of free monomer changes little with the total concentration: it is 8.3×10^{-5} M (note that the figure gives the mole fractions) at a total concentration of 17.5×10^{-5} M, *i.e.* when there are about equal amounts of free and micellized surfactant (in the calculations all species with aggregation number larger than unity are regarded as micelles), and increases to 9.2×10^{-5} M at 0.058 M total surfactant. The cmc should be close to the former value. The aggregation number changes perhaps more than what is normally expected, from 28 at twice the cmc to 75 at 58 mM. This is a feature that depends on the parameter values B_1 and B_2 and could be modified, but it should also be noted that the value presented is the number average over all species from the dimers. The aggregation number of the maximum in the micelle size distribution, as well as higher averages, grows much quicker initially, to a slowly changing plateau value.

The model with the large repulsive interactions gives different behavior. The concentration of free monomer is much larger, and the aggregation numbers are much smaller. At a total concentration of 2.4 mM the free monomer concentration is 1.4 mM and increases, but not dramatically, to 1.7 mM at a total concentration of about 20 mM (which would correspond to nearly 20 % w/w for $C_{12}E_{230}$). The average aggregation number grows more gradually in this range, from 4.9 to 14.1; the micelle size distribution is broad.

Although the free monomer concentration changes rather modestly even below 2.4 mM, there is no distinct cmc in this system. As the results are presented, there is no distinct cmc in the curves for $C_{12}E_8$ either, but in a linear representation, such a point can be easily localized, giving a cmc of about 8×10^{-5} M. The best construction for $C_{12}E_{230}$ would give cmc $\approx$ 1.4 mM; at this concentration the average aggregation number is just below 3.

We have also tried to model the aggregation of a compound with two alkyl ends, Figure 18. In this calculation, the formation of flower micelles from open unimers was considered. The full hydrophobic effect from the insertion of two tails into the core was used, and a back-bending penalty, estimated as in eq 19 was added. The resulting parameter values are given in the figure legend. In this case, the association is extremely gradual, with no sign of a cmc. Already at the lowest concentration considered, about 3.8×10^{-5} M, more of the polymer is associated than is present as free unimer (an additional population of unimers in loop conformation does not alter this statement). At low concentrations the association is open, with the dimer as the most abundant species. A maximum in the micelle size distribution does not appear until the total concentration is about 0.5 mM; the maximum then appears at an aggregation number of 8 (*i.e.* 16 chain ends). The average aggregation number is about 7 at this point and grows smoothly over the whole range.

A striking result from the calculations is the abundance of dimers, trimers, and other oligomeric aggregates, which are usually not found in the association of normal surfactants. The reason is simply that the concentration of free monomer reaches values which are not accessible in systems where large aggregates form. Although the free-energy model may be particularly bad in the region of small aggregation numbers, the general tendency for an initial open aggregation should be correct when strong repulsion pushes the aggregates toward the small size region and prevents an early micellization.

We now consider whether association behavior of this type would be consistent with the fluorescence and fluorescence quenching result obtained for pyrene in $C_{12}EO_{460}C_{12}$ solutions. The I/III results, as given in Figure 2, depend both on the fraction of pyrene present in a nonpolar environment and on how polar this environment is. The results for $C_{12}E_6$ show that a concentration of 0.1 mM of surfactant in the form of normal large micelles is enough for complete solubilization of pyrene in the micelles. Small micelles with an aggregation number on the order of 20 (tails) are much less favorable as solubilization vehicles,[43,44] and it is quite possible that a surfactant concentration larger by 1 order of magnitude would be required for a similar degree of solubilization. The oligomeric aggregates would probably not take up hydrophobic solutes, but even at low concentrations the open association process suggested by the model for the di-C_{12} polymer gives a substantial amount of micelles containing more than, *e.g.* 10 tails; such aggregates could take up the hydrophobic solutes and maybe even become stabilized in doing so. We could, therefore, expect an effect on the I/III values already at very low concentrations, but a complete transfer of pyrene to small micellar aggregates first occurs when the concentration of polymer in this form approaches 1 mM. The results in Figure 2 indicate that at this concentration the I/III ratio for $C_{12}EO_{460}C_{12}$ stabilizes at a level which indicates a more polar environment than a normal surfactant micelle, as would prevail in a small micelle.

To summarize: The change of the I/III values mirrors the transfer of pyrene from water to sufficiently large hydrophobic aggregates. In a system with an aggregation behavior as that modeled, the results cannot be used to determine a cmc, since there is no cmc. In the transition region a decreasing fraction, but increasing amount, of the polymer is in the form of small aggregates, that do not solubilize pyrene appreciably, whereas the concentration of free polymer must be much lower.

The results of the fluorescence quenching measurements cannot be used to calculate meaningful aggregation numbers, if the aggregation behavior is as the model suggests. The fluorescence decay curves serve to determine the fraction of (excited) pyrene molecules which are present in micelles without quencher. The number of aggregates follows if it is assumed that both pyrene and the quencher are Poisson-distributed over the micelles, and to obtain the aggregation number, the amount of polymer in aggregates must be known. The last problem was discussed above; it is also obvious that the Poisson distribution cannot be valid in a system like that modeled. Both pyrene and the hydrophobic quencher would associate primarily with the large micelles; they would probably avoid the oligomeric aggregates (but to different degrees). Furthermore, it is quite possible that pyrene and the quencher either avoid or prefer to be in the same micelles. Under these circumstances there is no valid way to calculate an average aggregation number from the apparent aggregation numbers; changes in the latter from measurements at different quencher concentrations signal deviations from Poisson distribution, but cannot be used reliably to determine the weight-average aggregation number and the micelle size distribution, since the principal reasons for the deviations from the Poisson distribution are not known.

If the principal features of the aggregation process are correctly captured by the model, then the fair (and sad!) conclusion must be that the aggregation numbers from the fluorescence quenching measurements are not meaningful. The results based on the quenching constants are still informative; however, most probes and quenchers are in aggregates which are much smaller than normal micelles and vary little in size with the polymer concentration. In addition there is probably a broad and varying distribution of micelles or aggregates of smaller size, all the way down to dimers, but not large amounts of larger micelles.

As stressed above, the model has several questionable features and should be regarded mainly as an illustration. It is possible that the real system behaves more like a normal micellar system, although with a much higher cmc and smaller micelles than expected for a species with two C_{12} tails, as suggested by the fluorescence results.

One aspect of the results is clear: the I/III results mark a range where extensive formation of micellar aggregates occurs, but this "cmc" is not a measure of the concentration of free unimers. A molecule with two C_{12} tails does not remain free in aqueous solution at a concentration close to 1 mM, and an aggregation of some kind should occur. In the model, the repulsive interactions come only from the corona, and as remarked above, these repulsive components are most probably exaggerated by the model function for low aggregation numbers. It is hard to see that any other interactions would hinder an aggregation into oligomeric aggregates.

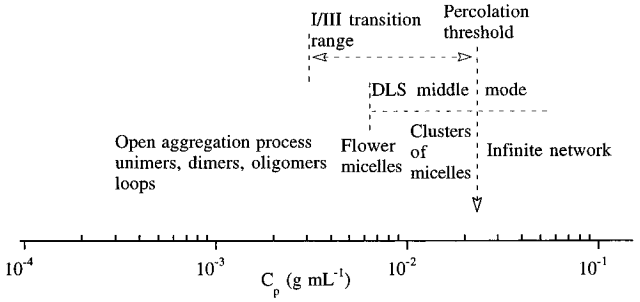

Figure 19. Schematic representation of the association process.

It is possible, however, that the aggregates with aggregation numbers of 15−30 are more stable than in the model, which would make the oligomeric aggregates less competitive and could give the aggregation process a more distinct appearance. Better stability would result if the repulsive interactions were less important than assumed in this region and if the strong increase of the free energy of the corona occurred first at higher aggregation numbers. Furthermore, the interfacial free energy of the core may decrease faster with the aggregation number than assumed, due to the fact that the alkyl groups at the interface become exposed to an environment where an increasing fraction of water is replaced by PEO, with more favorable interactions with the hydrocarbon. The stability of these intermediate aggregates could not be much larger than in the model, however, since the start of micelle-like aggregation would then occur at a much lower concentration.

Formation of the Network. The viscosity and DLS results are compatible with—or cannot disprove—an aggregation process as that discussed and summarized in Figure 19. The initial open aggregation process is followed by formation of flower micelles, which connect into a network already at a concentration of $C_p \approx (2-2.5) \times 10^{-2}$ g mL^{-1} by bridging interactions. The sharp rise of the viscosity at higher concentrations indicates a percolation threshold at this point; *i.e.* this would be the concentration where an infinite network of interconnected micellar nodes first appears. It is of some interest to consider the concentration of nodes required for its appearance.

It was noted above that the intermediate mode from DLS, in the concentration region just below C_p had a diffusion constant corresponding to a hydrodynamic radius which could be that of a flower micelle, about 110 Å. Micelles connected by bridging polymers should be separated by about twice this distance at low concentrations. Imagine a bcc lattice spanning the space, with a nearest-neighbor distance of 220 Å between the nodes. The percolation threshold in a bcc lattice appears when the fraction of occupied sites is 0.246, according to Stauffer et al.,[69] which corresponds to a concentration of occupied lattice points of ca. 5×10^{-5} M (about the same result is obtained with a simple cubic lattice, with percolation at 0.3116). It would be required that 25 polymers, $M_w = 20\,000$, were associated in each node for that concentration to correspond to $C_p = 2.5 \times 10^{-2}$ g mL^{-1} or (1.25×10^{-3} M). If a large fraction of the polymer is present as oligomeric aggregates that presumably have less tendency to participate in the network, or otherwise impose a shorter bridging distance, this number may be greatly reduced. For small aggregates, the end-to-end distance of the monomer (ca. 150 Å) may be used for the lattice point separation, giving instead 1.6×10^{-4} M and 8 for the

concentration at the threshold and the number of polymers per node, respectively. The aggregation numbers from the fluorescence measurements are between these limits.

The percolation threshold is where an infinite cluster is first formed. At the threshold the infinite cluster is highly ramified, with an infinite structural correlation length and there is, in addition, a broad distribution of smaller clusters all the way down to single micelles. The infinite cluster becomes more uniform, and the correlation length decreases with increasing concentration. Far above the threshold, the network is more uniform but contains a distribution of holes (with solvent but almost free from polymer), a swiss cheese type of structure, according to Stauffer et al.[69] The slow relaxation mode above the threshold can be understood to reflect the diffusion of finite clusters and holes, which of course is strongly slowed down as the network becomes denser. The dynamics of end-group association/dissociation in the hydrophobic nodes should be important in this connection. The disengagement time of a C_{12} alkyl chain from a normal micelle can be estimated to be of the order of 0.1 ms[70] or less and, even if several such events would be required to decouple a part of a cluster and allow it to be displaced, they could certainly influence a relaxation mechanism lying in the range of tens of milliseconds.

Conclusions

The main conclusions of the investigations presented above are summarized in Figure 19 where the different crossover regions are indicated according to the experimental methods of investigation. At very low concentrations, $C_p < 10^{-3}$ g mL^{-1}, most polymer molecules are free, some of which are closed to loops, or present in small oligomeric aggregates. Our measurements cannot distinguish between these forms. In pure water, less than 2% of the chains are included in large aggregates which seem to originate from chain−chain associations according to a mechanism suggested for PEO and other water-soluble polymers. These aggregates can be eliminated by addition of salt. For $C_p > 3 \times 10^{-3}$ g mL^{-1}, the presence of hydrophobic micelle-like microdomains is shown by the decrease of the I/III ratio of the pyrene fluorescence. The average aggregation number of these microdomains could not be determined with certainty; it seems to be around 15−30 (tails) and varies little with concentration. There are probably, in addition, many much smaller aggregates; the fraction of polymer in those would decrease with concentration. At $C_p > 7 \times 10^{-3}$ g mL^{-1}, dynamic light scattering shows the formation of aggregates with a diffusion coefficient 2.5 times lower than that of the free molecules. The overlap and bridging of these entities can be considered as responsible for the abrupt viscosity rise starting at $C_p \approx 2 \times 10^{-2}$ g mL^{-1}.

Acknowledgment. This work has been supported by grants from the Swedish National Board for Industrial and Technical Development (NUTEK). The authors would like to thank G. Beinert and F. Isel for their participation in the synthesis work. G. Svensk and S. Maitre are thanked for viscosity measurements. P. Hansson and E. Mukhtar are thanked for their assistance with the fluorescence measurements. S. Abrahmsén-Alami is acknowledged for stimulating discussions. J.F. would like to thank PIRMAT for financial support.

References and Notes

(1) *Polymer in Aqueous Media*; Glass, J. E., Ed.; Advances in Chemistry 223; American Chemical Society: Washington, DC, 1989.
(2) *Polymer as Rheology Modifiers*; Schultz, D. N., Glass, J. E., Eds.; Advances in Chemistry Series No. 462; American Chemical Society Symposium: Washington, DC, 1991.
(3) *Water Soluble Polymers for Petroleum Recovery*; Back, J., Valint, P. L., Jr., Pace, S. J., Siano, D. B., Schulz, D. N., Turner, S. R., Eds.; Plenum Press: New York, 1986; Vol. 147.
(4) *Polymeric Materials Science and Engineering Proceedings*; Nae, H. N., Reichert, W. W., Eds.; ACS Division of Polymeric Materials, American Chemical Society: Washington, DC, 1989; Vol. 61.
(5) Karunasena, A.; Glass, J. E. *Prog. Org. Coat.* **1989**, *17*, 301.
(6) Jenkins, R. D. Ph.D. Dissertation, Lehigh University, Bethlehem, PA, 1990.
(7) Santore, M. M. Ph.D. Dissertation, Princeton University, Princeton, NJ, 1990.
(8) *The Function of Associative Thickeners in Water-borne Paints*; Huldén, M., Sjöblom, E., Boström, P., Eds.; XXI Fatipec Congress, Amsterdam, 1992.
(9) Huldén, M. *Colloid Surf. A* **1994**, *82*, 263.
(10) Binana-Limbelé, W.; Clouet, F.; François, J. *Colloid Polym. Sci.* **1993**, *271*, 748.
(11) Binana-Limbelé, W.; Clouet, F.; François, J. Unpublished results.
(12) Richey, B.; Kirk, A. B.; Eisenhart, E. K.; Fitzwater, S.; Hook, J. W. *J. Coat Technol.* **1991**, *63*, 31.
(13) Hansson, P.; Almgren, M. *Langmuir* **1994**, *10*, 2115.
(14) (a) Yekta, A.; Duhamel, J.; Brochard, P.; Adiwidjaja, H.; Winnik, M. A. *Macromolecules* **1993**, *26*, 1829. (b) Yekta, A.; Duhamel, J.; Adiwidjaja, H.; Winnik, M. A. *Macromolecules* **1995**, *28*, 956.
(15) Yekta, A.; Duhamel, J.; Adiwidjaja, H.; Brochard, P.; Winnik, M. A. *Langmuir* **1993**, *9*, 881.
(16) Maechling-Strasser, C.; François, J.; Clouet, F.; Tripette, C. *Polymer* **1992**, *33*, 627.
(17) Maechling-Strasser, C.; Clouet, F.; François, J. *Polymer* **1992**, *33*, 1021.
(18) Nyström, B.; Walderhaug, H.; Hansen, F. K. *J. Phys. Chem.* **1993**, *97*, 7743.
(19) Persson, K.; Abrahmsén, S.; Stilbs, P.; Walderhaug, H.; Hansen, F. K. *Colloid Polym. Sci.* **1992**, *270*, 465.
(20) Walderhaug, H.; Hansen, F. K.; Abrahmsén, S.; Persson, K.; Stilbs, P. *J. Phys. Chem.* **1993**, *97*, 8336.
(21) (a) *Hydrophobic Polymers*; Alami, E., Rawiso, M., Isel, F., Beinert, G., Binana-Limbele, W., François, J., Eds.; Advances in Chemistry Series 248; American Chemical Society: Washington, DC, 1995; Chapter 18. (b) François, J. *Prog. Org. Coat.* **1994**, *24*, 67.
(22) Abrahmsén, Alami, S.; Alami, E.; François, J. *J. Colloid Interface Sci.* in press.
(23) Higgins, J. S.; Dawkins, J. V.; Maghami, G. G.; Shakir, S. A. *Polymer* **1986**, *27*, 931.
(24) Abrahmsén-Alami, S.; Stilbs, P. *J. Phys. Chem.* **1994**, *98*, 6359.
(25) Persson, K.; Wang, G.; Olofsson, G. *J. Chem. Soc., Faraday Trans.* **1994**, *90* (23), 3555.
(26) Persson, K.; Bales, B. L. *J. Chem. Soc., Faraday Trans.* **1995**, *91* (17), 2863.
(27) Semenov, A. N.; Joanny, J. F., Khokhlov, A. R. *Macromolecules* **1995**, *28*, 1066.
(28) Annable, T.; Buscall, R.; Ettelaie, R.; Whittlestone, D. *J. Rheol.* **1993**, *37* (4), 695.
(29) Rawiso, M.; Maitre, S.; François, J. Manuscript in preparation.
(30) Alami, E.; Almgren, M.; Brown, W., submitted to *Macromolecules*.
(31) *The Chemistry of Excitation at Interfaces*; Thomas, J. K., Ed.; ACS Monograph No. 181; American Chemical Society: Washington, DC, 1984.
(32) Kalyanasundaran, K.; Thomas, J. K. *J. Am. Chem. Soc.* **1977**, *99*, 2039.
(33) Turro, N. J.; Yekta, A. *J. Am. Chem. Soc.* **1978**, *100*, 5951.
(34) Almgren, M.; Löfroth, J. E. *J. Colloid Interface Sci.* **1981**, *81*, 486.
(35) Almgren, M.; Hansson, P.; Mukhtar, E.; Van Stam, J. *Langmuir* **1992**, *8*, 2405.
(36) Infelta, P. P.; Grätzel, M.; Thomas, J. K. *J. Phys. Chem.* **1974**, *78*, 190.
(37) Tachiya, M. *Chem. Phys. Lett.* **1975**, *33*, 289.
(38) Infelta, P. P. *Chem. Phys. Lett.* **1979**, *61*, 88.

(39) Atik, S. S.; Nam, M.; Singer, L. A. *Chem. Phys. Lett.* **1979**, *67*, 75.
(40) Brown, W.; Schillen, K.; Almgren, M.; Hvidt, S.; Bahadur, P. *J. Phys. Chem.* **1991**, *95*, 1850.
(41) (a) Jakes, J. *Czech. J. Phys.* **1988**, *B38*, 1305. (b) *Laser Light Scattering in Biochemistry*; Johnsen, R. M., Brown, W., Harding, S. E., Sattelle, D. B., Bloomfield, V. A., Eds.; Royal Society of Chemistry: London, 1992; p 77.
(42) Gramain, Ph.; Libeyre, R. *J. Appl. Polym. Sci.* **1970**, *14*, 383.
(43) Almgren, M.; Grieser, F.; Thomas, J. K. *J. Am. Chem. Soc.* **1979**, *101*, 279.
(44) Hansson, P.; Almgren, M. Submitted to *J. Phys. Chem.*
(45) Almgren, M. *Adv. Colloid Interface Sci.* **1992**, *41*, 9.
(46) Bales, B. L.; Stenland, C. *J. Phys. Chem.* **1993**, *97*, 3418.
(47) Devanand, K.; Selser, J. C. *Macromolecules* **1991**, *24*, 5943.
(48) Benkhira, A.; Franta, E.; Rawiso, M.; François, J. *Macromolecules* **1994**, *27*, 3963.
(49) Casassa, E. *J. Polym. Sci.* **1965**, *A3*, 605.
(50) Rempp, P.; Strazielle, C.; Lutz, P. *Encycl. Polym. Sci. Eng.* **1987**, *9*, 183.
(51) Stockmayer, W. H.; Fixmann, M. *Ann. N.Y. Acad. Sci.* **1953**, *57*, 334.
(52) Kirkwood, J. G.; Risemann, J. *J. Chem. Phys.* **1978**, *16*, 565.
(53) Strazielle, C. *Makromol. Chem.* **1968**, *119*, 50.
(54) Polik, W. F.; Burchard, W. *Macromolecules* **1983**, *16*, 978.
(55) (a) Devanand, K.; Selser, J. C. *Nature* **1990**, *343*, 978. (b) Porsch, B.; Sundelöf, L.-O. *Macromolecules* **1995**, *28*, 7165.
(56) Brown, W. *Macromolecules* **1984**, *17*, 66.
(57) Fang, L.; Brown, W. *Macromolecules* **1990**, *23*, 3284.
(58) De Gennes, P. G. *C. R. Acad. Sci. Paris, Ser. 2* **1991**, *313*, 1117.
(59) Erlander, S. R. *J. Colloid Interface Sci.* **1970**, *34*, 53.
(60) Sartori, R.; Sepulveda, L.; Quina, F.; Lissi, E.; Abuin, E. *Macromolecules* **1990**, *23*, 3878.
(61) Mortensen, K.; Brown, W.; Jorgensen, E. B. *Macromolecules* **1994**, *27*, 5654.
(62) McCormick, C. L.; Nonaka, T.; Johnson, C. B. *Polymer* **1988**, *29*, 731.
(63) Hill, A.; Candau, F.; Selb, J. *J. Prog. Colloid Polym. Sci.* **1991**, *84*, 61.
(64) Ten Brinke, G.; Hadziioannou, G. *Macromolecules* **1987**, *20*, 486.
(65) Raspaud, E.; Lairez, D.; Adam, M.; Carton, J. P. *Macromolecules* **1994**, *27*, 2956.
(66) Evans, H. C. *J. Chem. Soc.* **1956**, *579*.
(67) (a) *The Hydrophobic Effect: Formation of micelles and biological membranes*; Tanford, C. H., Ed.; J. Wiley and Sons: New York, 1973. (b) *The Hydrophobic Effect*, 2nd ed.; Tanford, C. H., Ed.; J. Wiley and Sons: New York, 1980.
(68) *Intermolecular and Surface Forces*, 2nd ed.; Israelachvili, J., Ed.; Academic Press: New York, 1991.
(69) *Introduction to Percolation Theory*; Stauffer, D., Aharony, A., Eds.; Taylor and Francis: London, 1992.
(70) Aniansson, E. A. G.; Wall, S. N.; Almgren, M.; Hoffman, H.; Kielmann, I.; Ulbricht, W.; Zana, R.; Lang, J.; Tondre, C. *J. Phys. Chem.* **1976**, *80*, 905.

MA951174H